Int. J. Mar. Sci. Eng., 2 (2), 153-162, Spring 2012
ISSN 2251-6743

Comparison between linear and nonlinear models for surge motion of TLP

[1] M. R. Tabeshpour; [2] R. Shoghi*

[1]Center of Excellence in Hydrodynamics and Dynamics of Marine Vehicles, Mechanical Engineering Department, Sharif University of Technology; Tehran; Iran
[2] Professional Engineer, Tehran; Iran

Received 10 April 2012; revised 29 April 2012; accepted 11 May 2012

ABSTRACT: Tension-Leg Platform (TLP) is a vertically moored floating structure. The platform is permanently moored by tendons. Surge equation of motion of TLP is highly nonlinear because of large displacement and it should be solved with perturbation parameter in time domain. This paper compare the dynamic motion responses of a TLP in regular sea waves obtained by applying three method in time domain using MATLAB soft ware. In this paper Lindstedt- Poincare method (L-P method) is used to solve nonlinear differential equation of surge motion considering first-order perturbation. Also modified Euler method (MEM) is used for solving nonlinear equation of motion as numerical method and ordinary differential equation is used for linear equation of motion (without nonlinear term). The results were obtained as responses represent good accordance between results of L-P method and MEM.

Key words: *tension leg platform; surge motion; Morison equation; perturbation method*

INTRODUCTION

Compliant offshore structures are used for oil exploitation in deep water. The surge motion equation of tension leg platform has nonlinear term. The high nonlinear surge motion equation must be solved in time domain by rising force on TLP. The hydrodynamic forces are calculated using the Morison equation according to Airy's linear wave theory for different waves condition. The responses obtained from linear motion equation and those achieved from analytical method via perturbation method for nonlinear status are compared with numerical results. Perturbation techniques (Nayfeh, 1973; Kevorkian and Cole, 1981) are used to solve nonlinear motion equation in time domain. Many studies have been carried out to understand the structural behavior of a TLP and to determine the effect of several parameters on the dynamic response and average life time of the structure (Ahmad, 1996; Jain, 1997; Chandrasekaran and Jain, 2002). A comprehensive study on the results of tension leg platform responses in random seas, considering all structural and excitation nonlinearities, is presented by Tabeshpour *et al.* (2006). First order perturbation solution for axial vibration of tension leg platforms, is presented (Golafshani *et al*., 2007). An analytical heave vibration of a TLP with radiation and scattering effect for damped systems has been presented (Tabeshpour *et al*., 2006). Surge motion analysis of TLP under linear wave via perturbation method is presented (Tabeshpour and Shoghi, 2011). Many of the phenomena around us are inherently non-linear and are expressed or described as nonlinear equations. Since the advent of digital computers, each day is easier to solve linear equations and this is while there is no exact answer for many nonlinear equations. In many cases, finding

* Corresponding Author Email: tabeshpour@sharif.edu
rahim_shoghi@yahoo.com

the analytical solution of nonlinear equations is much more difficult than obtaining the numerical solutions. But now with advances in computer hardware and having very powerful software such as Maple, Mathematica and MATLAB which are working with symbolic variables it is getting easy to solve the most of equations. Generally numerical solution of nonlinear equations can be obtained by sophisticated computer calculations. In comparison to numerical method, easier solution of non-linear problems is advantage of analytical solution. Essentially all physical systems are nonlinear. Most of assumptions and approximations are presented in way that mathematical problem governing the behavior of the system is linear. Because solving linear problem is much easier than nonlinear one. Because the superposition is not applicable in nonlinear systems, Analysis of nonlinear systems is very complicated in comparison to linear systems. Consequently in nonlinear system:

1- Homogeneous Solving of nonlinear differential equation of second order, is not obtained from combination of the two independent linear solution.

2- The general solution of nonlinear differential equations cannot be written as the sum of the particular and homogeneous solutions, which is independent of initial conditions.

3- The linear combination cannot be used for adding forced response to combination of stimulations.

4- Because convolution integral is calculated by using a principle superposition, it cannot be used for nonlinear systems. There is no equivalent to the convolution integral in nonlinear systems.

5- The Laplace transform cannot be used to obtain the solution of nonlinear differential equations.

MATERIALS AND METHODS

Equation of Motion

Structural modeling of a TLP as a moored structure is shown in Fig. 1. Because the buoyancy of the TLP exceeds its weight, the vertical equilibrium of the platform requires taut moorings connecting the upper structure to the seabed. The extra buoyancy over the platform weight ensures that the tendons are always kept in tension.

T_0 is Initial pre-tension in tethers. By giving an arbitrary displacement, x, in the surge direction (see Fig. 2), the increase in the initial pre-tension in each leg is given by:

$$\Delta T = k_0(\sqrt{l_0^2 + x^2} - l_0) \ , \qquad (k_0 = A_t E / l_0) \tag{1}$$

$$\sin\theta = x / \sqrt{l_0^{\ 2} + x^2} \tag{2}$$

$$F_s \approx T_0 + 0.5 k_0 x^2 / l_0 \tag{3}$$

where:

x: displacement in the surge direction,

θ: angle between the initial and the displaced position of the tether,

l_0: initial length of each tether,

E: Young's modulus of the tether,

F_s: tension of tendon,

k_0: axial stiffness of tether,

ΔT: increase in the initial pre-tension due to the arbitrary displacement and

A_t: cross-sectional area of tether.

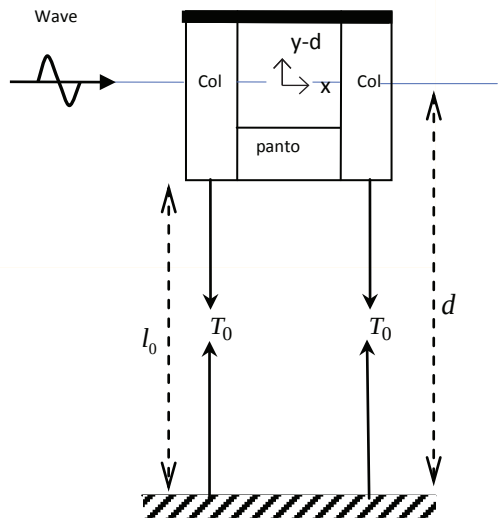

Fig. 1: TLP as a moored structure

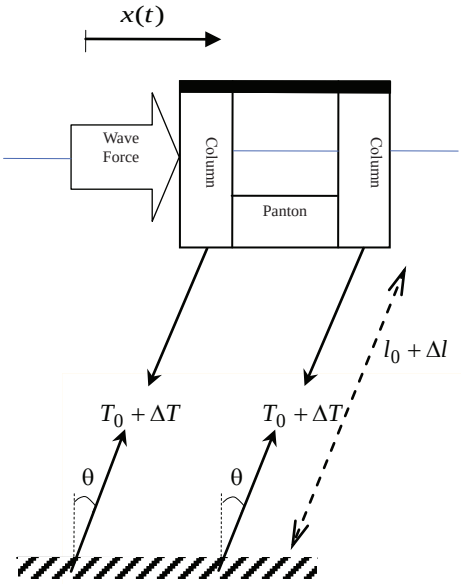

Fig. 2: TLP by given arbitrary displacement

Considering equilibrium equation of surge motion the equation of motion in x direction under wave take the form of:

$$\sum F_x = M_{st}\ddot{x} \tag{4}$$

$$M_{st}\ddot{x} + c\dot{x} + F_s \sin(\theta) = F_{wave} \tag{5}$$

Substituting Eqs. (2) and (3) into Eq. (5), one obtains:

$$M_{st}\ddot{x} + (T_0 + n\frac{k_0 x^2}{2l_0})(\frac{x}{l_0})(1+\frac{x^2}{2l_0^2})^{-1} = F_{wave} \tag{6}$$

n is number of tendon.In the above equation Structural damping is assumed to be equal to zero and one can be approximated that by Eq. (7).

$$M_{st}\ddot{x} + (\frac{T_0}{l_0})x + (\frac{nk_0}{2l_0^2})x^3 = F_{wave} \tag{7}$$

or

$$M_{st}\ddot{x} + k_1 x + k_3 x^3 = F_{wave} \tag{8}$$

That $k_1 = T_0 / l_0$ and $k_3 = nk_0/(2l_0^2)$, where M_{st}, k_1 and k_3 are structural mass, linear and nonlinear stiffens parameter, respectively. Fig. 3 represents mechanical modeled of TLP under harmonic force.

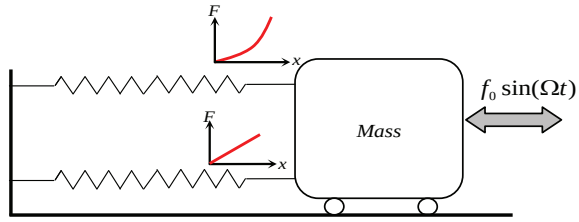

Fig. 3: Structural modeling of TLP considering hardening spring

That Structural damping is assumed to be equal to zero. By giving an arbitrary displacement in the x direction, the forces in the each term of spring take the form of below. For linear and non-linear force are as follow, respectively.

$$F_{spring}^{(L)} = k_1 x \tag{9}$$

$$F_{spring}^{(NL)} = k_3 x^3 \tag{10}$$

The amount of elastic force for a given displacement is expressed as follows:

$$F_{spring} = k_1 x + k_3 x^3 \tag{11}$$

k_3 is very small quantity rather than k_1, while nonlinear force due to nonlinear stiffness, $k_3 x^3$, is remarkable in comparison to linear force, $k_1 x$. In the following fig., the linear and nonlinear force of tendon versus displacement is shown.

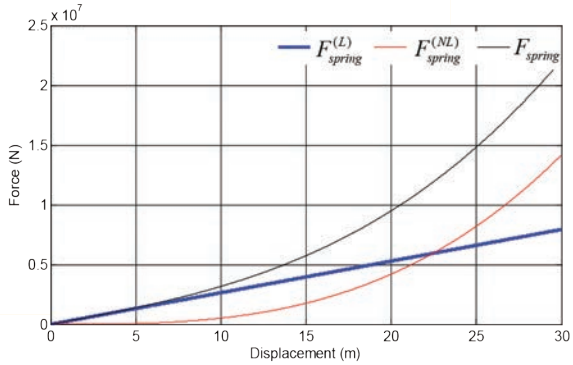

Fig. 4: horizontal tendon force versus displacement

The potential energy function due to the presence of x^4 is not parabolic shape. Different forms of power and potential in below figure for systems with large displacement (worked in non-linear) are shown.

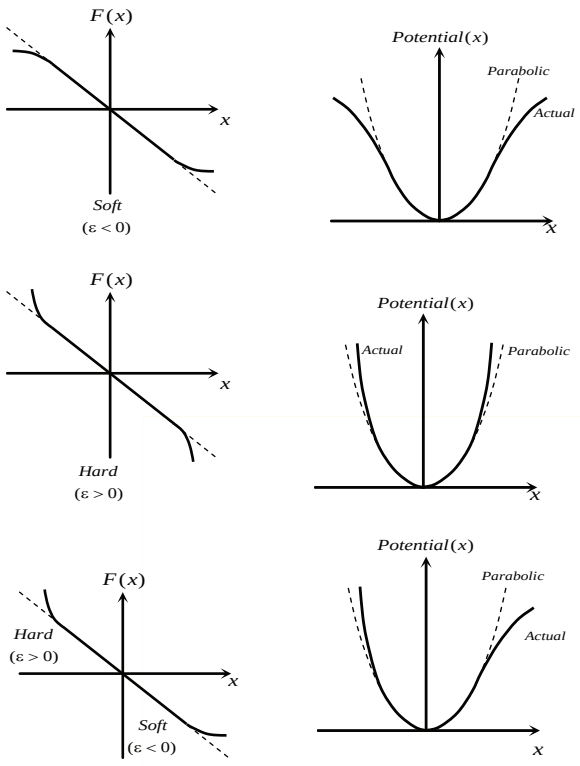

Fig. 5: power and potential figure for systems with large displacement

If the spring is loaded with a force, Fig. 6a, and its deflection is measured then a force-displacement curve can be generated, such as that of Fig. 6b. Typically, the curve is a straight line for small range of force (linear range). The slope of this line is a constant called the stiffness coefficient of the spring *k*. Beyond the linear regime, the spring shows a nonlinear force- displacement relationship characterized by either increasing in stiffness (hardening behavior) or decreasing in stiffness (softening behavior) compared to the linear case.

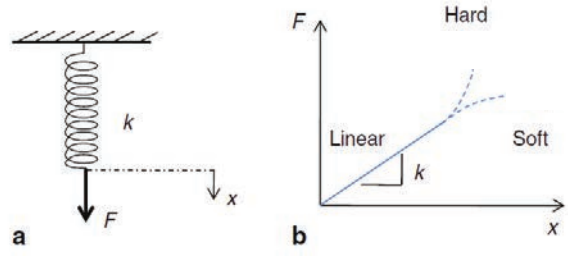

Fig. 6 a: A schematic shows a spring being pulled by a force. b- A force- displacement curve showing a linear regime with a slope k ending with a possible nonlinear hardening or softening behaviours

In the following figure, considering $k_3/k_1 = 0.002$, the influence of nonlinear term on large displacement is shown.

$$F_{spring} = k_1 x + k_3 x^3 = k_1 x(1 + \frac{k_3}{k_1} x^2) \quad (12)$$

$$\frac{F_{spring}}{F_{Linear}} = \frac{k_1 x(1 + \frac{k_3}{k_1} x^2)}{k_1 x} = 1 + \frac{k_3}{k_1} x^2 \quad (13)$$

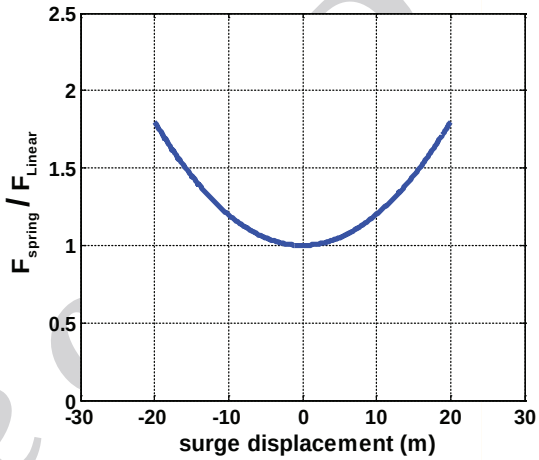

Fig. 7: proportion of total force to linear force

Wave force:

Wave force determination is significant for the design of an offshore structure. The geometry of the structure i.e. the ratio of size to the wave length, the hydrodynamic parameters and the rigidity of the structure, affect the wave load experienced by the structure. Depending on the type and size of the structure, different wave load determination approaches may need to be applied. Morison equation is applicable to a structure, which is small comparative to the wave length. The inertia and drag coefficients need to be determined experimentally and are considered as a constant usually. Values of inertia and drag coefficients are resented in below:

Table 1: values of inertia and drag coefficients

	Smooth		Rough	
	C_d	C_m	C_d	C_m
API	0.65	1.6	1.05	1.2
SNAME	0.65	2.0	1.0	1.8

Morison equation was established as the basis of wave load determination for offshore structures due to the simplicity of the implementation and programming. The existence of the structure will affect the wave field surrounding the structure. However, when the size of structure relative to the wave length is greater than 0.2, Morison Equation is no longer applicable. Also the current effect was evaluated using the drag term of Morison equation. The linear Airy wave theory and Morison equation were used for the determination of the wave kinematics and wave force respectively. Also Morison equation expressed the wave force as a summation of inertia force and drag force. The water particle kinematics was determined by the following equations:

$$\xi(t,x)=\frac{H}{2}\cos(kx-\Omega t) \tag{14}$$

$$k=2\pi/L \tag{15}$$

The horizontal water particle velocity and acceleration at the vertical centerline of a circular cylinder at x = 0 are given by:

$$u(x,t)=\frac{\pi H}{T}\frac{\cosh ky}{\sinh kd}\cos(kx-\Omega t) \tag{16}$$

$$\dot{u}(x,t)=\frac{2\pi^2 H}{T^2}\frac{\cosh ky}{\sinh kd}\sin(kx-\Omega t) \tag{17}$$

Relation between k,Ω and h are observed in follow equation:

$$\omega^2=gk\tan hkd \tag{18}$$

that y is vertical direction origin of sea bed, x is surge direction, H is wave height, L is wave length, ξ is wave level, Ω is wave frequency, u is water particle velocity, $\dot{u}$ is water particle acceleration and k is wave number. In deep water, $d/L>0.5$, follow equation is used replace Eq. (18).

$$L=gT^2/(2\pi) \tag{19}$$

Morison, *et al.* introduced a semi-intuitive equation to compute wave forces on elements immersed objects having characteristic dimensions that are small compared to the wavelength of the incident wave. Also it was observed in most of the reported studies that Morison equation was employed in the calculation of the wave loads to determine the dynamic responses for this structure. Wave forces due to sea wave on the members of TLP, calculated by Morison equation on TLP columns as below:

$$F_{morison}=\sum(F_{inertia}+F_{drag})_{column} \tag{20}$$

Assuming that the force coefficients C_m and C_d are constants and integrating over the still water depth On columns yields:

$$F_{morison}=\sum_{column}\left(\iiint C_m\rho\dot{u}\,d\nu-\iiint C_a\rho\ddot{x}\,d\nu+\int\frac{C_d\rho}{2}|u-\dot{x}|(u-\dot{x})dy\right) \tag{21}$$

$$m_{add}=\iiint C_a\rho\ddot{x}\,d\nu \tag{22}$$

that C_m, C_a and C_d are inertia, added mass and drag coefficient m_{add} added mass on TLP columns and ν is volume of column. Substituting Eq. (22) into Eq. (21) one can be obtained:

$$F_{morison}=\sum_{column}\left(\iiint C_m\rho\dot{u}\,d\nu+m_{add}+\int_{y_1}^{y_2}\frac{C_d\rho}{2}|u-\dot{x}|(u-\dot{x})dy\right) \tag{23}$$

Ignoring the drag force and substituting Eq. (23) into Eq. (8), one obtains:

$$\left(M_{st}+\sum_{column}m_{add}\right)\ddot{x}+k_1x+k_3x^3=\sum_{column}\iiint C_m\rho\dot{u}\,d\nu \tag{24}$$

Substituting Eqs. (17) into Eq. (24) one can be obtained:

$$\left(M_{st}+\sum_{column}m_{add}\right)\ddot{x}+k_1x+k_3x^3=\sum_{column}\left(C_m\rho\frac{2\pi^2H}{T^2}0.25\pi D_c^2\int_{y_1}^{y_2}\frac{\cosh ky}{\sinh kd}\sin(kx-\Omega t)dy\right) \tag{25}$$

y_1 and D_c are bottom level and diameter of columns and y_2 is still water level. The Morison equation may be integrated for a total depth-integrated force on a vertical circular cylinder by applying linear wave theory kinematics:

$$\left(M_{st}+\sum_{column}m_{add}\right)\ddot{x}+k_1x+k_3x^3=\sum_{column}\left(\frac{C_m\rho2\pi^2H0.25\pi D^2}{T^2\sinh kd}\left(\frac{\sinh ky_2-\sinh ky_1}{k}\right)\right)\times\sin(kx-\Omega t) \tag{26}$$

$$\ddot{x}+\omega_n^2x+\varepsilon x^3=\sum_{column}\left(\frac{C_m\rho2\pi^2H}{T^2\sinh kd}\frac{0.25\pi D_c^2(\sinh ky_2-\sinh ky_1)}{k\left(M_{st}+\sum_{column}m_{add}\right)}\right)\times\sin(kx-\Omega t) \tag{27}$$

that $\omega_n^2=k_1/(M_{st}+\sum_{column}m_{add})$ and $\varepsilon=k_3/(M_{st}+\sum_{column}m_{add})$.

$$F=\sum_{column}\left(C_m\rho\frac{2\pi^2H}{T^2\sinh kd}\frac{0.25\pi D_c^2(\sinh ky_2-\sinh ky_1)}{k\left(M_{st}+\sum_{column}m_{add}\right)}\right) \quad (28)$$

The surge motion equation can be written as:

$$\ddot{x}+\omega_n^2x+\varepsilon x^3=F\sin(kx-\Omega t) \quad (29)$$

Considering origin of x on column $x=0$ one can be obtained:

$$\ddot{x}+\omega_n^2x+\varepsilon x^3=F\sin(\Omega t) \quad (30)$$

Where F, ω and ε are the amplitude of wave, frequency of wave force and perturbation parameter respectively. L-P method is used to solve Eq. (30).

Solving methods

Lindstedt- Poincare method (L-P method):

Forced vibration equation of motion is as follows:

$$\ddot{x}+\omega_n^2x+\varepsilon x^3=F\sin(\Omega t) \quad (31)$$

Perturbation method is used to solve Eq. (31). A solution in the form of an infinite series of the perturbation parameter ε is assumed as follows:

$$x(t)=x_0(t)+\varepsilon x_1(t)+\varepsilon^2x_2(t)+\varepsilon^3x_3(t)+... \quad (32)$$

In this method the frequency of nonlinear vibration depends on the perturbation parameter:

$$\omega^2=\omega_n^2+\varepsilon\alpha_1+\varepsilon^2\alpha_2+\varepsilon^3\alpha_3+... \quad (33)$$

where α_i are as yet undefined functions of amplitude. In this study, the first-order perturbation method is used to solve the differential equation, therefore the response and frequency of vibration are considered as follow:

$$x(t)=x_0(t)+\varepsilon x_1(t), \quad (34)$$

$$\omega^2=\omega_n^2+\varepsilon\alpha_1. \quad (35)$$

Substituting Eqs. (34) and (35) into Eq. (31), one obtains:

$$(\ddot{x}_0+\varepsilon\ddot{x}_1)+(\omega^2-\varepsilon\alpha_1)(x_0+\varepsilon x_1)+\varepsilon(x_0+\varepsilon x_1)^3=F\sin(\Omega t) \quad (36)$$

Since the perturbation parameter ε could have been chosen arbitrarily, the coefficients of the various powers of ε must be equated to zero. This leads to a system of equations which can be solved successively:

$$\ddot{x}_0+\omega^2x_0=F\sin(\Omega t), \qquad x_0(0)=\dot{x}_0(0)=0 \quad (37)$$

$$\varepsilon\ddot{x}_1+\omega^2x_1-\alpha_1x_0+x_0^3=0, \qquad x_1(0)=\dot{x}_1(0)=0 \quad (38)$$

The solution of Eq. (37), subjected to the initial conditions $x_0(0)=0$ and $\dot{x}_0(0)=0$ is:

$$x_0=\frac{F}{\omega^2-\Omega^2}(\sin\Omega t-\frac{\Omega}{\omega}\sin\omega t) \quad (39)$$

Substituting Eq. (39) into the right-hand side of Eq. (38), one obtains:

$$\ddot{x}_1+\omega^2x_1=\alpha_1\frac{F}{\omega^2-\Omega^2}(\sin\Omega t-\frac{\Omega}{\omega}\sin\omega t) -\left(\frac{F}{\omega^2-\Omega^2}\right)^3\times\left\{\begin{array}{l}\sin^3\Omega t-\left(\frac{\Omega}{\omega}\right)^3\sin^3\omega t\\ -\left(\frac{3\Omega}{\omega}\right)\sin^2\Omega t\sin\omega t-3\left(\frac{\Omega}{\omega}\right)^3\sin^2\omega t\sin\Omega t\end{array}\right\}, \quad x_1(0)=\dot{x}_1(0)=0 \quad (40)$$

Using:

$$\sin^2\theta=0.5(1-\cos2\theta) \quad (41\text{-a})$$

$$\sin(\theta_1t)\cos(\theta_2t)=0.5(\sin(\theta_1-\theta_2)t+\sin(\theta_1+\theta_2)t) \quad (41\text{-b})$$

$$\sin^3\theta=0.75\sin\theta-0.25\sin3\theta \quad (41\text{-c})$$

Eq. (40) can be rewritten as:

$$\ddot{x}_1+\omega^2x_1=-\alpha_1\frac{F}{\omega^2-\Omega^2}(\sin\Omega t-\frac{\Omega}{\omega}\sin\omega t)- \left(\frac{F}{\omega^2-\Omega^2}\right)^3\times\left\{\begin{array}{l}\frac{3}{2}\left(\frac{1}{2}+\left(\frac{\Omega}{\omega}\right)^2\right)\sin\Omega t-\frac{1}{4}\sin3\Omega t\\ -\frac{3}{4}\left(\frac{\Omega}{\omega}\right)^3\sin\omega t+\frac{1}{4}\left(\frac{\Omega}{\omega}\right)^3\sin3\omega t\\ \frac{3\Omega}{4\omega}\left(\sin(\omega-2\Omega)t+\sin(\omega+2\Omega)t\right)\\ -\frac{3}{4}\left(\frac{\Omega}{\omega}\right)^2\left(\sin(\Omega-2\omega)t+\sin(\Omega+2\omega)t\right)\end{array}\right\}, \quad x_1(0)=0,\dot{x}_1(0)=0 \quad (42)$$

The forcing term $\sin(\omega t)$ leads to a secular term $t\sin\omega t$ in the solution of x_1. Such terms violate the initial stipulation that the motion is to be periodic. Therefore one must impose the following condition:

$$\alpha_1=0.75(\Omega/\omega)^2\left(F/(\omega^2-\Omega^2)\right)^2 \quad (43)$$

And Substituting Eq. (43) into Eq. (35), the vibration frequency becomes:

$$\omega^2=\omega_n^2+0.75\varepsilon(\Omega/\omega)^2(F/(\omega^2-\Omega^2))^2 \quad (44)$$

The frequency is found to increase with ε, as expected because of increasing axial stiffness of tether.

$$R = F/(\omega^2 - \Omega^2) \tag{45}$$

considering $D_1 = \alpha R - 1.5R^3(0.5 + (\Omega/\omega)^2)$, $D_2 = R^3/4$ $D_3 = -0.25(R\Omega/\omega)^3$, $D_4 = D_5 = 0.75R^3(\Omega/\omega)^2$ and $D_6 = D_7 = 0.75R^3(\Omega/\omega)$. also $\phi_1 = \Omega$, $\phi_2 = 3\Omega$, $\phi_3 = 3\omega$, $\phi_4 = (\omega - 2\Omega)$, $\phi_5 = (\omega + 2\Omega)$, $\phi_6 = (\Omega - 2\omega)$, $\phi_7 = (\Omega + 2\omega)$. Considering Eq. (42) is as follows:

$$\ddot{x}_1 + \omega^2 x_1 = \sum_{i=1}^{7} D_i \sin(\phi_i t), \quad x_1(0) = 0, \ \dot{x}_1(0) = 0 \tag{46}$$

Now imposing the initial conditions $x_1(0) = 0, \dot{x}_1(0) = 0$, the homogenous solution of Eq. (46) is as follow.

$$x_1^{(h)} = C_1 \sin(\omega t) + C_2 \cos(\omega t) \tag{47}$$

The particular solution of Eq. (46) is:

$$x_1^{(p)} = \sum_{i=1}^{7} d_i \sin(\phi_i t) \tag{48}$$

where $d_i = D_i/(\omega^2 - \phi_i^2)$. Now the solution of Eq. (46) is as follows:

$$x_1(t) = x_1^{(h)} + x_1^{(p)} = C_1 \sin(\omega t) + C_2 \cos(\omega t) + \sum_{i=1}^{7} d_i \sin(\phi_i t) \tag{49}$$

Imposing the initial conditions $x_1(0) = 0$, $\dot{x}_1(0) = 0$, results are

$$x_1(0) = 0 \rightarrow C_2 = 0 \tag{50}$$

$$\dot{x}_1(0) = 0 \rightarrow C_1\omega + \sum_{i=1}^{7} d_i\phi_i = 0 \rightarrow C_1 = -\frac{1}{\omega}\sum_{i=1}^{7} d_i\phi \tag{51}$$

consuming $d_0 = C_1$ and $\phi_0 = \omega$, now the solution of Eq. (46) is as follows:

$$x_1(t) = \sum_{i=0}^{7} d_i \sin(\phi_i t) \tag{52}$$

Substituting Eqs. (52) and (39) into Eq. (34), the first-order perturbation solution of Eq. (31) becomes:

$$x(t) = x_0(t) + \varepsilon\sum_{i=0}^{7} d_i \cos(\phi_i t) \tag{53}$$

The modified Euler method (MEM)

Euler method is rarely used but knowing it is a starting point toward further examination of the methods of this class. The graphic presentation is shown in Fig. 9. There is a known point of coordinates (y_m, x_m) lying on the wanted curve. A curve with a slope is drawn through this point

$$y'_m = f(x_m, y_m) \tag{54}$$

We can assume that y_{m+1} equals to the ordinate at the crossing point of L_1 and the straight line $x = x_{m+1} = x_m + h$. The equation of the straight line L_1 is:

$$y = y_m + y'_m(x - x_m) \tag{55}$$

and since $x_{m+1} - x_m = h$ then:

$$y_{m+1} = y_m + h(x_m - y_m) \tag{56}$$

The error in $x = x_{m+1}$ is designated on the figure by *e*. The last formula assigns the Euler method. Its characteristic is the big error from disruption and instability in some cases, i.e. a small error from rounding increases with the increase of *x*. The modified Euler method is based on finding the average value of the slopes of the tangent lines in the points (x_m, y_m) and $(x_m + h, y_m + hy'_m)$. Graphically the method is presented on Fig. 10.

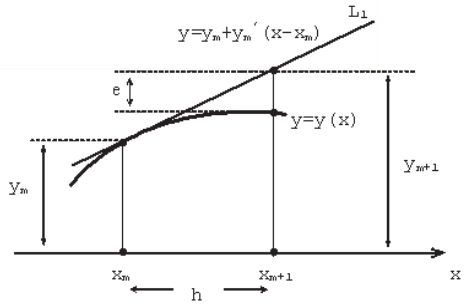

Fig. 8: Geometric presentation of Euler method

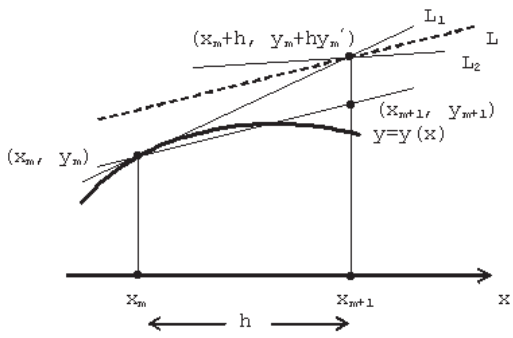

Fig. 9: Geometric presentation of the MEM

The slope of the straight line L is:

$$\Phi(x_m, y_m, h) = \frac{1}{2}\left[f(x_m, y_m) + f(x_m + h, y_m + hy'_m) \right] \quad (57)$$

where $y'_m = f(x_m, y_m)$. The equation for L is assigned as:

$$y = y_m + (x - x_m)\Phi(x_m, y_m, h) \quad (58)$$

$$y_{m+1} = y_m + h\Phi(x_m, y_m, h) \quad (59)$$

The last equations express the MEM.

RESULTS AND DISCUSSION

A numerical study has been carried out to understand the effect of parameters ε and the amplitude of vibration. The period of the structure is about equal to 77 second, therefore the linear frequency of system is $\omega_n = 0.0812$ rad/s, and the initial conditions are $x(0) = 0$ and $\dot{x}(0) = 0$ imposed. The Table 2 represents the character of TLP for compare of results.

Table 2: Character of square TLP

characters	symbol	value	dimension
weight	M_{st}	209500	*kN*
Buoyancy	F_b	334000	*kN*
pre-tension	T_0	124500	*kN*
Columns diameter	D_c	14.2	*m*
Panton diameter	D_P	11	*m*
TLP length	P_b	58.3	*m*
Tendon diameter	D	0.4	*m*
Tendon length	l	471	*m*
Tendon stiffness	k	58060	*kN/m*
Water depth	d	500	*m*
Number of leg	n	4	-
Inertia coefficient	C_m	2	-
Water density	ρ	1024	kg/m^3

Table 3 represent the maximum displacement of motion for values of wave period $T_{wave} = 8s$ and different wave heights, increasing in amplitude force due to wave height, the maximum response is measured by different methods.

Table 3: obtained errors between linear and l-p method comparing mem

$T_{wave} = 8\ s$					
$H\ (m)$	Maximum surge response (m)			Error %	
	Linear	L-P method	MEM	Linear & MEM	L-P & MEM
8	3.45	3.42	3.45	0	<1
10	4.32	4.26	4.29	0.69	<1
12	5.19	5.12	5.13	1.16	<1
14	6.05	5.94	5.97	1.34	<1
16	6.91	6.77	6.79	1.76	<1

Above table shows that the difference between linear method and MEM for all assumed wave heights is less than 9% and the difference between L-P method and MEM is less than 1% which shows good agreement between L-P method and MEM and their difference with linear status.

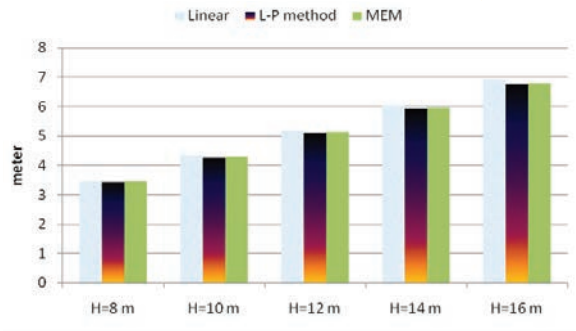

Fig. 10: Obtained response amplitude by different method for Twave=8 s

Fig. 10 represent response obtained from linear method is clearly more than MEM responses. It is due to ignoring of hardening nonlinear term which leads to decreasing the response amplitude. Also the obtained responses from L-P method have very good agreement with the numerical method discussed. Table 4 represent the maximum displacement of motion for values of wave period $T_{wave} = 10s$ and different wave heights,

increasing in amplitude force due to wave height, the maximum response is measured by different methods.

Table 4: obtained errors between linear and l-p method comparing mem

$T_{wave} = 10\ s$					
$H\ (m)$	Maximum surge response (m)			Error %	
	Linear	L-P method	MEM	Linear & MEM	L-P & MEM
8	8.71	8.45	8.5	2.47	<1
10	10.88	10.41	10.43	4.31	<1
12	13.08	12.35	12.38	5.65	<1
14	15.25	14.19	14.23	7.16	<1
16	17.42	15.95	15.99	8.94	<1

Above table shows that the difference between linear method and MEM for all assumed wave heights is less than 9% and the difference between L-P method and MEM is ever less than 1% which shows good agreement between L-P method and MEM and their difference with linear status.

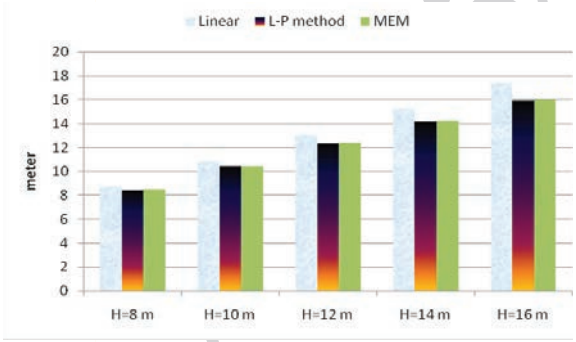

Fig. 11: Obtained response amplitude by different method for Twave=10 s

Fig. 11 represent response obtained from linear method is clearly more than MEM responses. It is due to ignoring of hardening nonlinear term which leads to decreasing the response amplitude. Also the obtained responses from L-P method have very good agreement with the numerical method discussed. Table 5 represent the maximum displacement of motion for values of wave period $T_{wave} = 12\,s$ and different wave heights,

increasing in amplitude force due to wave height, the maximum response is measured by different methods.

Table 5: obtained errors between linear and l-p method comparing mem

$T_{wave} = 12\ s$					
$H\ (m)$	Maximum surge response (m)			Error %	
	Linear	L-P method	MEM	Linear & MEM	L-P & MEM
8	15.49	14.41	14.59	6.16	1.23
10	19.35	17.50	17.7	9.32	1.12
12	23.24	20.43	20.86	11.40	2.06
14	27.12	23.14	22.5	20.53	2.84
16	30.76	22.65	24.59	25.09	7.88

Above table shows that the difference between linear method and MEM for all assumed wave heights is less than 25% and the difference between L-P method and MEM is less than 8% which shows good agreement between L-P method and MEM and their difference with linear status.

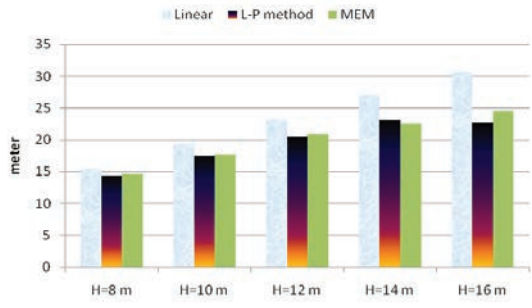

Fig. 12: Obtained response amplitude by different method for Twave=12 s

Fig. 12 represent response obtained from linear method is clearly more than MEM responses. It is due to ignoring of hardening nonlinear term which leads to decreasing the response amplitude. Also the obtained responses from L-P method have very good agreement with the numerical method discussed. Fig. 13 represents errors obtained between linear method and L-P method comparing MEM. Increase in wave period and wave height causes the governing equation

of TLP motion to be more nonlinear and linear method not to be applicable in this status.

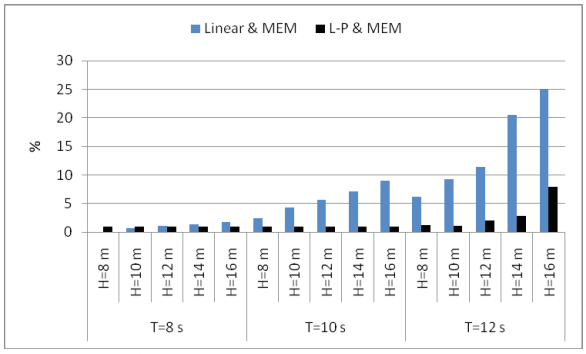

Fig. 13: Obtained error

Obtained errors from linear method are clearly more than L-P method in above mentioned status.

CONCLUSION

Equation of surge motion of TLP is highly nonlinear under large displacement because of nonlinear stiffness. When displacement of TLP is small, linear differential equation of TLP is applicable as governing equation of TLP motion and has the same result for three discussed methods. Also, so long as mass displacement doesn't cause remarkable increase in nonlinear spring force in comparison to linear spring force the L-P method has very good agreement with the numerical method. Increasing in amplitude of response to cause error obtained from linear method is clearly more than L-P method. According to this paper, the procedures can be repeated considering damping effect for free and forced vibration cases.

REFERENCES

Ahmad, S., (1996). Stochastic TLP Response Under Long crested Random Sea. journal of computers and structures, 61 (6), 975-993.

Chandrasekaran, S.; Jain, A.K., (2002). Dynamic Behavior of Square and Triangular Offshore Tension leg platform Under regular Wave Loads. Journal of Ocean engineering, 29, 279-313.

Golafshani, A. A.; Tabeshpour, M. R.; Seif, M. S., (2007). First Order Perturbation Solution for Axial Vibration of Tension leg plat forms. Journal of Scientia Iranica, 14, 414-423.

Jain, A.K., (1997). Nonlinear Coupled Response of Offshore Tension leg platforms to Regular Wave Forces. Journal of Ocean engineering, 24 (7), 577-592.

Kevorkian, J.; Cole, J. D., (1981). Perturbation Methods in Applied Mathematics, New York: Springer.

Nayfeh, A. H., (1973). Perturbation Methods. New York-John Wiley & Sons.

Tabeshpour, M.R.; Golafshani, A. A.; Seif, M.S., (2006). Comprehensive Study on the Results of Tension leg platform Responses in Random Sea. Journal of Zhejiang University, 7, 1305-1317.

Tabeshpour, M .R.; Golafshani, A. A.; Ataie ashtiani, B.; Seif, M. S., (2006). Analytical Solution of Heave Vibration of Tension leg platform. Journal of Hydrology and Hydromechanics, 54 (3), 280-289.

Tabeshpour, M. R.; Shoghi, R., (2011). Surge motion analysis of TLP under linear wave via perturbation method, offshore industries conference. Iran.

How to cite this article: (Harvard style)

Tabeshpour, M. R.; Shoghi, R., (2012). Comparison between linear and nonlinear models for surge motion of TLP. Int. J. Mar. Sci. Eng., 2 (2), 153-162.